Sensors and Materials, Vol. 36, No. 8 (2024) 3211–3225
MYU Tokyo

S & M 3728

Reproduction of Absorption Spectra of Bromothymol Blue–Methyl Red Mixed Indicator from RGB and L*a*b* Color Coordinates and Application to Fast Spectrum Acquisition

Yusuke Kimura, Arinori Inagawa,* and Nobuo Uehara

Faculty of Engineering, Utsunomiya University, 7-1-2 Yoto, Utsunomiya, Tochigi 321-8585, Japan

(Received October 11, 2023; accepted February 14, 2024)

Keywords: color coordinates, spectrum reproduction, millisecond spectroscopy, nonequilibrium system

The RGB-spectral conversion method has been used to quantitatively visualize proton diffusion phenomena that occur in a time on the order of 10 ms when an acidic ion-exchange resin is placed on an agar gel containing an acid-base indicator. The absorption spectra of the mixed indicator of bromothymol blue and methyl red were reproduced from two sets of color coordinates: RGB and L*a*b* values. We recorded a video of the color change of bromothymol blue–methyl red (BTB–MR)-containing agar gel in contact with the ion-exchange resin at a time interval of 10 ms. We successfully obtained the absorption spectra in a short time and predicted the pH values around the resin. Our results suggest that the spectral conversion method based on color coordinates has the potential for measuring the behavior of materials in nonequilibrium systems. Moreover, the present method would be one of the novel sensing technologies for the continuous monitoring of spectral change, which can be utilized as precise inline analysis.

1. Introduction

Microspectroscopy has enabled the measurement of physical properties in a small area by using various spectroscopic techniques under a microscope.[1,2] Numerous targets have been measured by microspectroscopy, such as living cells[3] and components in mineral resources.[4] Recent advances in microfluidic technologies have enabled the chemical reaction in micro-nanospaces to be controlled.[5,6] To evaluate the reaction process therein, the fast and position-dependent acquisition of spectral information is required. In general, microspectroscopy involves a microscope, a light source, a spectrometer, and a detector. A diffraction grating is typically used as a spectrograph in spectroscopic measurements, which require a certain amount of time to scan a wide range of wavelengths. However, this makes it difficult to obtain spectral data in millisecond (ms) times. In recent years, the development of hyperspectral imaging systems has made it possible to acquire the spectral information of a target material. However, the conventional scanning method of hyperspectral imaging does not allow snapshot imaging,

*Corresponding author: e-mail: ainagawa@cc.utsunomiya-u.ac.jp
https://doi.org/10.18494/SAM4699

ISSN 0914-4935
https://myukk.org/

where position-dependent spectral information is acquired instantaneously.[7] Hyperspectral imaging is typically performed by repeating 1D line scans or by successively replacing optical filters or changing the angle of the grating. Therefore, both methods require the imaging of a fixed object for a fixed period of time, and there is a need for both non-grating and non-scanning spectroscopy systems that can acquire instantaneous spectral information to realize high-speed spectral measurement in microspectroscopy.

The use of color coordinates is one possible solution to overcome the above problem. Most digital color images contain spectral data in the form of RGB values. However, the RGB values are defined as overlapping integrals of the spectral intensities of the incident and transmitted/reflected lights, and the spectral sensitivity of the color filter. Therefore, they cannot be treated as true spectral data. There have been numerous attempts to reproduce spectral information from color coordinates. Smits reported an algorithm for RGB spectrum conversion to ensure the reproducibility of color on graphic displays.[8] Although the method is instantaneous, the reproducibility is poor for chemical analysis because the display only requires three colors to produce all colors, meaning that spectral resolution is less important. Our research group has developed an RGB-spectral conversion method to reproduce the absorption spectra of a material in a short time.[9–13] The loading and score vectors obtained by the principal component analysis (PCA) and expansion of the spectra and the RGB values obtained from the microscopic image of the standard solution are used to calculate a conversion matrix that is linearly related to the RGB and score values. This conversion matrix enables the reproduction of absorption spectra from the RGB values of microscopic images of solutions. We have applied these approaches to the measurement of pH in a frozen aqueous solution, to proton diffusion phenomena at the aqueous two-phase interface in microfluidic devices,[9] and to a method of total protein quantification using smartphone images.[13] Our previous studies have demonstrated its potential to simplify and improve the accuracy of spectroscopic measurements. As mentioned above, the RGB spectrum conversion method has been investigated in various ways by reproducing the absorption spectrum of an instant from a single snapshot. If this method can be applied to the reproduction of absorption spectra using snapshots taken continuously in ms times by the RGB-spectral conversion method, it should be possible to elucidate the behavior of materials from their spectral changes. Moreover, the application of the present methodologies to video data enables the continuous monitoring of the chemical species based on spectrophotometry with a simple experimental setup, which would be one of the novel sensing technologies.

In our previous study, we established a method for applying the RGB-spectral conversion method to ms measurements.[14] We quantitatively visualized the proton diffusion phenomena occurring when an ion-exchange resin containing a pH indicator is placed on a gel with concentrations set to 0.5 and 0.1 wt%. The gel network regulates the mass transportation therein. The elucidation of mass transportation in a gel is important to understand the behavior of the substances therein, because gels not only exist in living creatures but are also used as delivery systems in medicine and nutrition. As the transporting substance, we employed protons because they are easily detected. In our previous studies, the spectrum of a pure pH indicator was reproduced by the conversion method. The pH indicator used was bromothymol blue (BTB), whose absorption spectra were reproduced by the 10 ms conversion method. However, the

applicable pH range was limited because the color change of BTB generally occurs in the pH range of 6–8. Moreover, the proton transportation behavior in the 0.1 wt% gel was not monitored well because the low concentration increased the rate of proton diffusion. Herein, a quasi-universal indicator, which is a mixture of BTB and methyl red (MR), was used to extend the measurable pH range. We employed MR because of its discoloration pH range of 4.8–6.0[15] and because the color of BTB overlaps that of MR in the acidic range. MR is extensively used in various universal pH indicators for the above reasons.[16] The spectrum was reproduced using six color coordinates comprising RGB and L*a*b* values. Similarly, pH values at the gel/ion-exchange resin interface were calculated from the reproduced absorption spectra. This study is the first attempt to reproduce the spectra of mixed species. The results of this study demonstrate the versatility and feasibility of the present method, which can be applied to more complex solution systems.

2. Experimental Section

2.1 Reagents

BTB and MR were purchased from FUJIFILM Wako Pure Chemical Co. (Japan). Ethanol, hydrochloric acid, ammonium acetate, sodium hydroxide, and agarose were purchased from Kanto Chemical Co. (Japan). An ion-exchange resin (Amberlite™ FPC240H) was purchased from Organo Co. (Japan). All aqueous solutions were prepared using ultrapure water purified with a PURELAB Ultra Ionic system (ELGA Labwater, UK). All chemicals were used as received.

2.2 Sample preparation

The BTB–MR mixed indicator was prepared by the following procedure: First, 0.1047 g of BTB was dissolved in 100 mL of 50 vol% aqueous ethanol to obtain a 1.7×10^{-3} mol L^{-1} BTB solution. Next, 0.1005 g of MR was dissolved in 90 vol% aqueous ethanol to obtain a 3.7×10^{-4} mol L^{-1} MR solution. The mixed indicator was prepared by mixing 10 mL of the 1.7×10^{-3} mol L^{-1} BTB solution, 10 mL of the 3.7×10^{-4} mol L^{-1} MR solution, and 80 mL of ultrapure water. For the pH standard solution, 1 mL of 1.0 mol L^{-1} ammonium acetate solution and 1 mL of the BTB–MR mixture were mixed in a beaker. The solution pH was adjusted with 1.0 mol L^{-1} sodium hydroxide solution and 1.0 mol L^{-1} hydrochloric acid. After the pH adjustment, the mixture was made up to 10 mL in a volumetric flask.

2.3 Spectral measurement and data analysis

The absorption spectra of the BTB standard solutions were measured using a UV-visible spectrophotometer (V-750, JASCO, Japan) in a 1 cm cuvette. A series of acquired spectra were analyzed using MATLAB (MathWorks, USA) to obtain the score values and loading vectors.

2.4 Image acquisition setup

Digital color images of the samples were acquired using a microscope (SZM223T, AS ONE, Japan) equipped with a CMOS camera (MU-503, AmScope, USA). The samples were poured into a handmade glass cuvette. Both standard and gel solutions were poured into a circular cell chamber with a height of 1 mm and a radius of 1 cm. The agarose solutions were poured immediately after heating, before gelation occurred upon cooling. The top of each sample was flattened with a glass slide. For the gel samples, the glass slides were removed after gelation. This resulted in thin gel samples of 1 mm thickness. To monitor proton diffusion, a single ion-exchange resin was carefully placed on the gel surface using a micromanipulator. The diffusion was monitored by video at a time interval of 10 ms. All experiments were conducted in a dark room with the temperature set to 25 °C. During the image acquisition, white light was irradiated with an LED light source, which was originally equipped in the microscope and was set above the sample.

2.5 Procedure for reproducing absorption spectra

The mathematical background of the procedure for reproducing absorption spectra was described in our previous papers.[9,11,12] When a series of absorption spectra $\boldsymbol{A}$ are analyzed by PCA, the loading vector $\boldsymbol{L}$ and score vector **S** are obtained. The relationship between $\boldsymbol{A}$, $\boldsymbol{S}$, and $\boldsymbol{L}$ can be expressed as

$$\boldsymbol{A} = \boldsymbol{SL}. \tag{1}$$

The loading vector is universal when the same indicator is used throughout the experiment. Thus, if score values can be obtained from the color coordinates by calculation, absorption spectra can be reproduced by multiplying the calculated score values and the loading vectors. To determine the relationship between the color coordinates and the score values experimentally, both the color coordinates and score values of the standard pH solution containing the BTB–MR indicator were obtained. The digital color images were acquired using the microscope equipped with the digital camera, and color information was obtained using ImageJ. Herein, we utilized RGB and L*a*b* color coordinates. Simultaneously, absorption spectra of the standard solution were obtained using the spectrophotometer and analyzed by PCA. The conversion matrix $\boldsymbol{X}$ was then experimentally determined by the least-squares method using

$$\begin{pmatrix} s_1 & s_2 & \cdots & s_n \end{pmatrix} = \begin{pmatrix} R & G & B & L^* & a^* & b^* \end{pmatrix} \boldsymbol{X}, \tag{2}$$

where n is the number of loading vectors and R, G, B, L^*, a^*, and b^* are the RGB values actually obtained from the microscopic image of the solution. Therefore, $\boldsymbol{X}$ has dimensions of $6 \times n$.

2.6 Quantitative visualization of proton diffusion at gel/ion-exchange resin interface using RGB-spectral conversion method

We added 1 mL of the BTB–MR mixed solution, 0.0010 g of agarose, and 5 μL of 0.05 mol L^{-1} NaOH to a 10 mL beaker and heated it on a hot plate to dissolve and prepare a BTB–MR-containing agarose gel. A single particle of the ion-exchange resin, which was regenerated with 1.0 mol L^{-1} HCl, was placed on the agarose gel. Proton diffusion phenomena were monitored every 10 ms for 1500 ms with the digital camera. RGB values over an area of 35 × 35 μm^2 at four points 140 μm from the side of the ion-exchange resin were obtained from the color images.

3. Results and Discussion

3.1 Determination of conversion matrix X_{BTB-MR} to reproduce absorption spectra of BTB–MR mixed solution

The absorption spectra of a BTB–MR solution measured with a spectrophotometer are shown in Fig. 1(a). The height of the peak at 435 nm increases with the concentration of protonated BTB in the solution, whereas the height of the peak at 620 nm increases with the concentration of deprotonated BTB. The height of the peak at 500 nm also increases with the concentration of

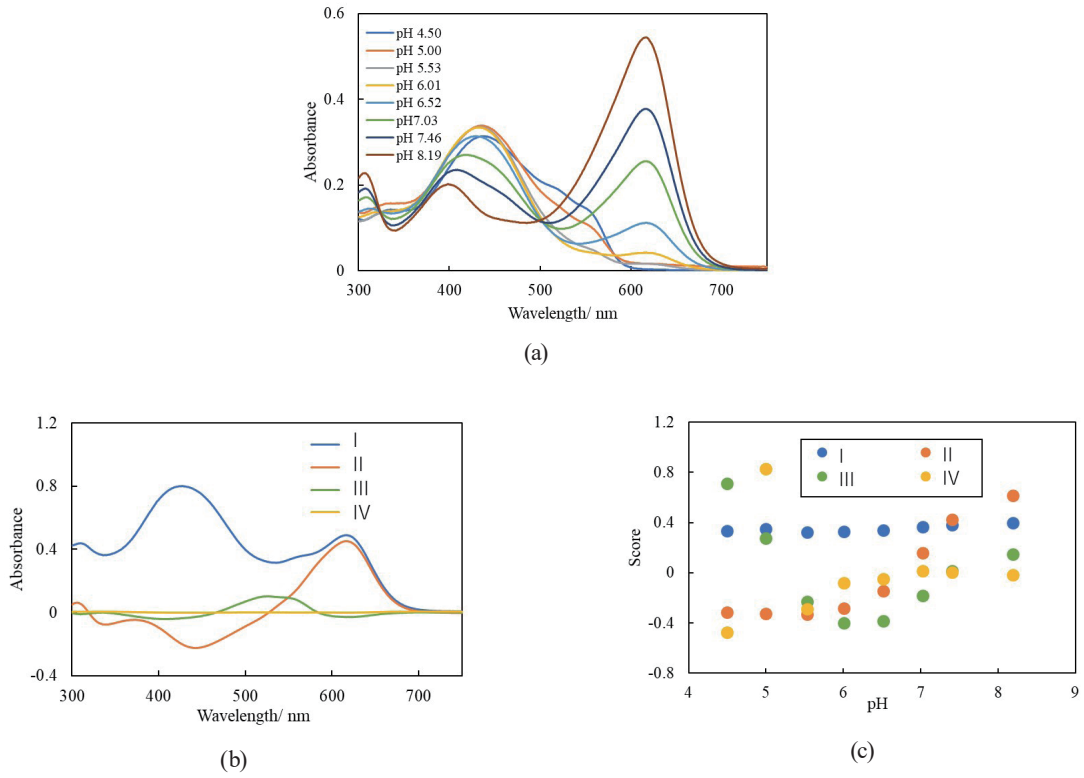

Fig. 1. (Color online) Absorption spectra of pH standard solution containing BTB−MR mixed indicator solutions obtained by PCA: (a) absorption spectra, (b) loading vectors, and (c) score values.

protonated MR. Therefore, up to four principal components were considered in PCA. The absorption spectra were examined by PCA. The conversion matrix $\boldsymbol{X}_{BTB-MR}$ was determined using six components of color information: the three components of the RGB system plus the three components of the L*a*b* color system. The loading matrix and score values obtained by PCA for this absorption spectrum are shown in Figs. 1(b) and 1(c), respectively. The eigenvalues of each component of the standard BTB–MR mixture obtained by PCA are shown in Table 1. The eigenvalue of the spectral series, which was mean-centered, was calculated with MATLAB software. Although the number of chemical species involved in the spectral change is considered to be four, namely, protonated BTB, proton-dissociated BTB, protonated MR, and proton-dissociated MR, we found that the spectral series consisted of only three loading vectors. Although the fourth loading vector can be treated as noise, we include this component here to improve reproducibility. A microscopic image of the standard BTB–MR mixture obtained using a light microscope is shown in Fig. 2(a). The RGB values of this microscopic image are given in Fig. 2(b). Note that the blue color has a minimum value at pH 5.53. Since pH 5.53 is the middle

Table 1
Eigenvalue of each loading vector obtained by PCA.

	Loading vector I	Loading vector II	Loading vector III	Loading vector IV	Loading vector V
Eigenvalue	0.62	0.35	0.033	7.1×10^{-5}	2.3×10^{-5}

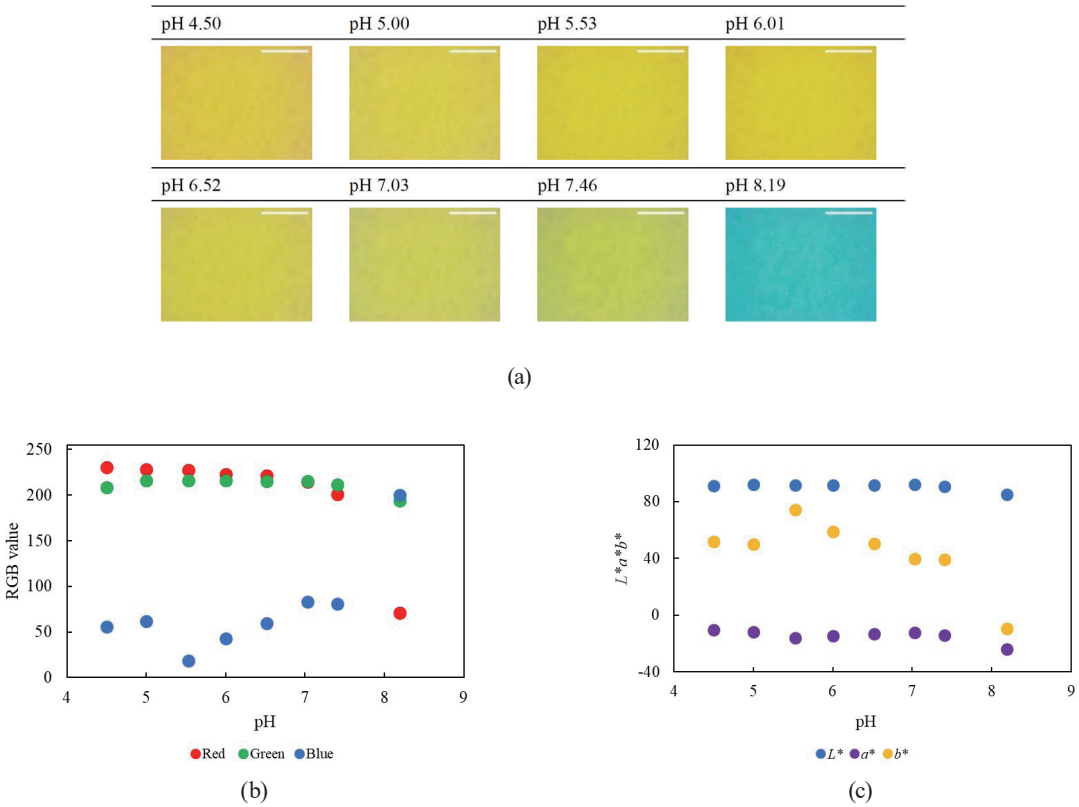

Fig. 2. (Color online) Image analysis of pH standard solution containing BTB−MR mixed indicator solutions: (a) digital color images, (b) RGB values, and (c) L*a*b* values.

point of the discoloration range of MR, MR starts to exhibit a yellowish color when pH increases, leading to the absorption of the blue color. Above this pH value, BTB also starts to produce blueish deprotonated species. Therefore, the blue value starts to increase. The RGB values were converted to the XYZ color space, and the L*a*b* values were calculated using this space. The L*a*b* values of the microscopic image of the standard BTB–MR mixture are given in Fig. 2(c).

The conversion equations used are as follows:

$$\begin{bmatrix} X \\ Y \\ Z \end{bmatrix} = \begin{bmatrix} 0.4124 & 0.3576 & 0.1805 \\ 0.2126 & 0.7152 & 0.0722 \\ 0.0193 & 0.1192 & 0.9505 \end{bmatrix} \begin{bmatrix} R \\ G \\ B \end{bmatrix}, \tag{3}$$

$$\begin{bmatrix} X_0 \\ Y_0 \\ Z_0 \end{bmatrix} = \begin{bmatrix} 0.4124 & 0.3576 & 0.1805 \\ 0.2126 & 0.7152 & 0.0722 \\ 0.0193 & 0.1192 & 0.9505 \end{bmatrix} \begin{bmatrix} 255 \\ 255 \\ 255 \end{bmatrix}, \tag{4}$$

$$L^* = 116 \times \left(\frac{Y}{Y_0} \right) - 16, \tag{5}$$

$$a^* = 500 \times \left\{ \left(\frac{X}{X_0} \right)^{\frac{1}{3}} - \left(\frac{Y}{Y_0} \right)^{\frac{1}{3}} \right\}, \tag{6}$$

$$b^* = 200 \times \left\{ \left(\frac{Y}{Y_0} \right)^{\frac{1}{3}} - \left(\frac{Z}{Z_0} \right)^{\frac{1}{3}} \right\}. \tag{7}$$

The conversion matrix $\boldsymbol{X}_{BTB–MR}$ determined by the RGB, L*a*b*, and score values is

$$X_{BTB–MR} = \begin{bmatrix} -0.0254 & -0.5231 & 0.0139 & 0.5038 \\ 0.0270 & 0.5411 & -0.1292 & -0.3747 \\ -0.0010 & -0.2202 & 0.0433 & 0.2047 \\ 0.0241 & 0.4672 & 0.2029 & -0.7590 \\ 0.1267 & 2.5726 & 0.0392 & -2.4582 \\ 0.0041 & 0.0656 & 0.0767 & -0.1095 \end{bmatrix}. \tag{8}$$

The $\boldsymbol{X}_{BTB–MR}$ conversion matrix has 6 × 4 dimensions, representing four-component score values with the six-component color information. Note that this $\boldsymbol{X}_{BTB–MR}$ is applicable whenever the same instrumentation setup is used, including the camera, incident light, and cell.

3.2 Calculation of coefficient of agreement between reproduced and measured absorption spectra of BTB–MR mixed solution

Figures 3(a)–3(c) show microscopic images, RGB values, and L*a*b* values of the BTB–MR mixture under the newly adjusted pH conditions, respectively. These color coordinates were converted to score values using $\boldsymbol{X}_{BTB-MR}$, the results of which are summarized in Fig. 3(d). The absorption spectra of BTB were then reproduced using the calculated score values, and the reproduced absorption spectra are shown in Fig. 4(a). The absorption spectra reproduced by Smits' method are also shown in Fig. 4(b), which was used to evaluate the reproducibility of the present method. We found that the absorption spectra reproduced by the present method are in good agreement with the shape of the measured absorption spectra measured with a spectrophotometer, as shown in Fig. 5(a). To quantitatively evaluate the reproducibility of the absorption spectra, the consistency factor f was determined from the absorption spectra measured with a spectrophotometer. f is defined as

$$f = \sqrt{\frac{\int \{A_s(\lambda) - A_r(\lambda)\}^2 d\lambda}{\int \{A_s(\lambda)\}^2 d\lambda}} \times 100, \tag{9}$$

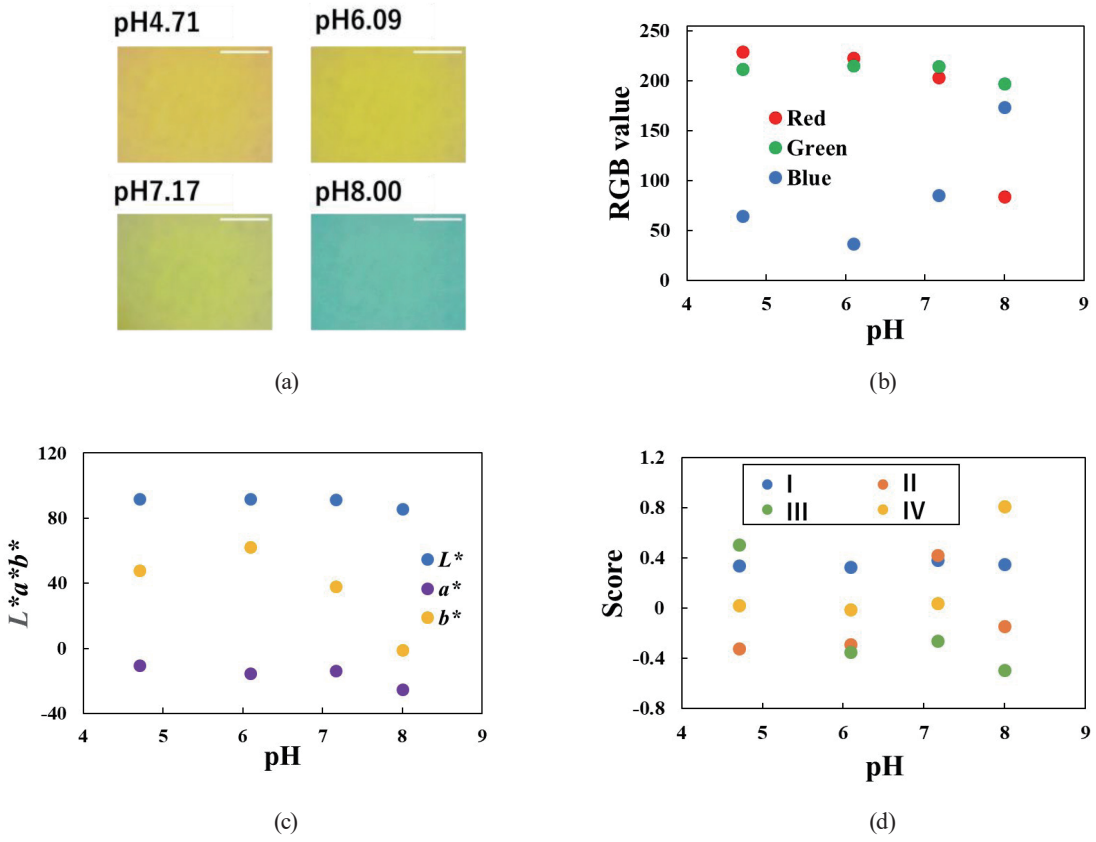

Fig. 3. (Color online) Image analysis of the BTB−MR solution for the reproduced absorption spectra: (a) digital color images, (b) RGB values, (c) L*a*b* values, and (d) score values obtained with the conversion matrix $\boldsymbol{X}_{BTB-MR}$.

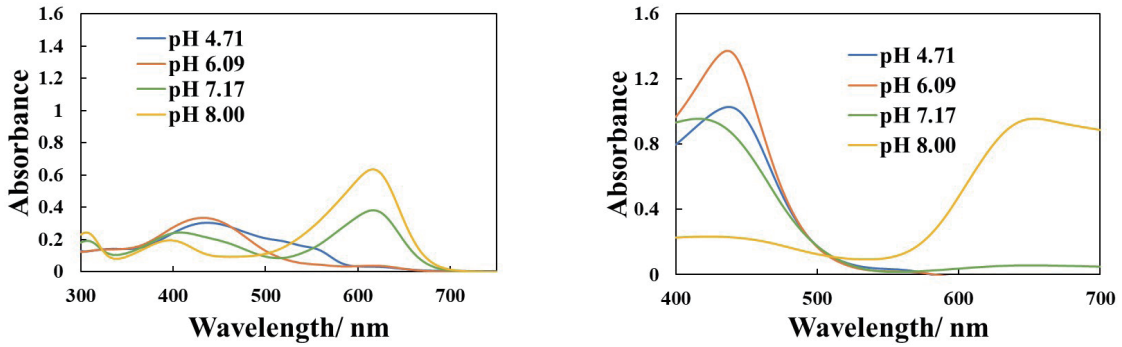

Fig. 4. (Color online) Reproduction of absorption spectra of BTB–MR solution with different pH values: absorption spectra reproduced by (a) the present method and (b) Smits' method.

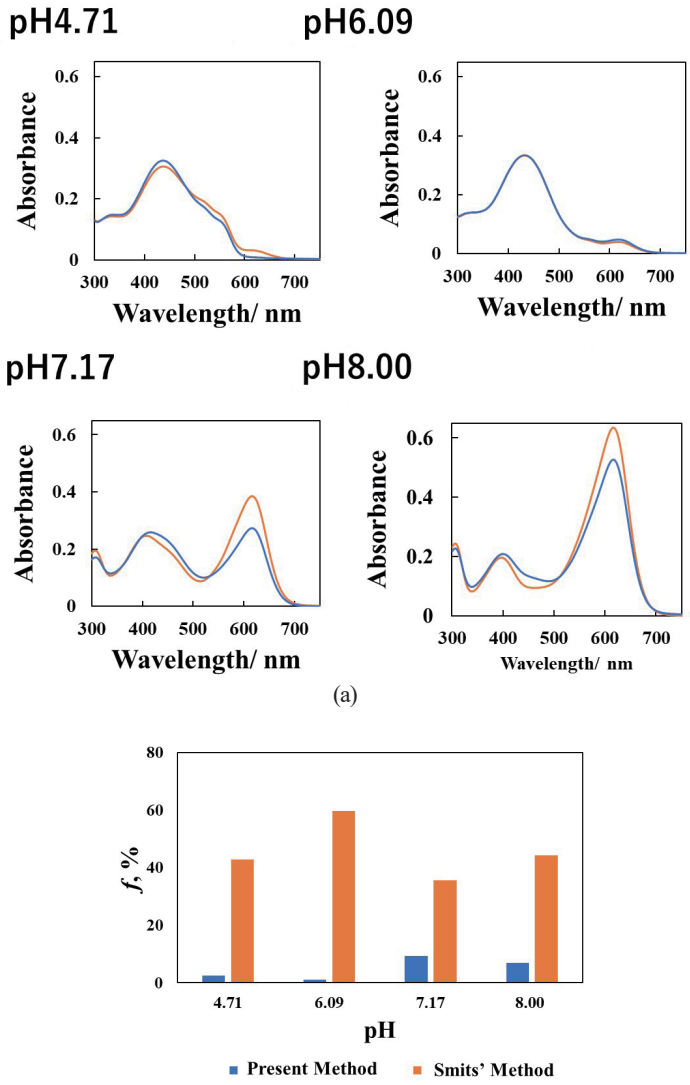

Fig. 5. (Color online) Comparison of the reproduced absorption spectra with the spectra measured with a spectrophotometer: (a) appearance (orange bar: reproduced spectra; blue bar: spectrophotometric spectra) and (b) f values for present method and Smits' method.

where A_s and A_r are the absorption spectra measured with the spectrophotometer and reproduced by the present method, respectively. When f is 0, the reproduced spectra are identical to the spectrophotometric spectra. The f values determined for the reproduced spectra are shown in Table 2. f was less than 10% for all pH values. In this study, the f values at higher pH values tended to be larger. In other words, the absorbance at longer wavelengths exhibited more variation. The opposite results were observed in our previous study.[9] This difference might have been caused by the optical properties of the white LED light. The f values for the spectra reproduced by Smits' method were also calculated, and the results are shown in Fig. 5(b). We found that the f values for the absorption spectra reproduced by Smits' method were 30–60%, which were larger than those for the present method, indicating the greater reproducibility of the present method for obtaining absorption spectra from color coordinates.

3.3 Quantitative visualization of proton diffusion phenomena at gel/ion-exchange resin interface

We used the present method to monitor proton diffusion from the ion-exchange resin placed on a low-concentration agarose gel containing BTB–MR indicators. Figure 6 shows optical microscopic images of proton diffusion at the interface between the gel and the ion-exchange resin. The RGB and L*a*b* values obtained from these images are shown in Figs. 7(a) and 7(b), respectively. The absorption spectra reproduced using the color coordinates and the conversion matrix $\boldsymbol{X}_{BTB-MR}$ are shown in Fig. 8. We confirmed that the spectral change was successfully detected by the present method. The divergence of the spectral series in the lower part is due to the shadow of the ion-exchange resin. To avoid this problem, the light path should be optimized, which will be addressed in a future study. The pH values were calculated from these spectra. Since a complex equilibrium calculation is required to determine pH values with the universal pH indicator, we employed a multiple regression equation to determine pH values from the specific absorbance indicated by absorption spectra reproduced by the present method. Multiple regression analysis was performed on the spectra of the standard mixture obtained with a spectrophotometer, and a regression curve for determining pH was calculated by substituting the absorbance at 436, 503, and 620 nm. Herein, the absorbance in Fig. 1(a) was used. From the regression analysis, the following equation was obtained:

$$\mathrm{pH} = 5.13 \times A_{\lambda 436} - 13.3 \times A_{\lambda 503} + 6.43 \times A_{\lambda 620} + 5.58. \tag{10}$$

The regression curve was first used to determine the pH of the aqueous BTB–MR solution. pH was adjusted to 4.71 using a pH meter, and microscopic images were taken every 10 ms for 1500 ms. The RGB and L*a*b* values of the microscopic images are shown in Figs. 9(a) and 9(b),

Table 2
f values for the reproduced absorption spectra.

	pH 4.71	pH 6.09	pH 7.17	pH 8.00
f (%)	2.6	1.0	9.3	6.9

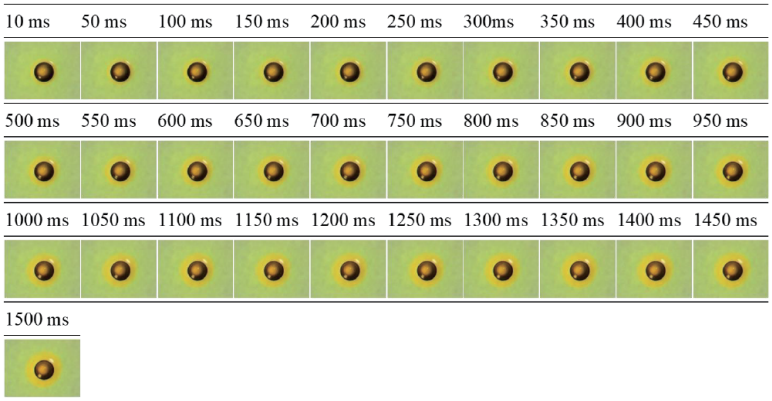

Fig. 6. (Color online) Digital color images of the proton diffusion from the ion-exchange resin to BTB−MR−containing 0.1 wt% agarose gel.

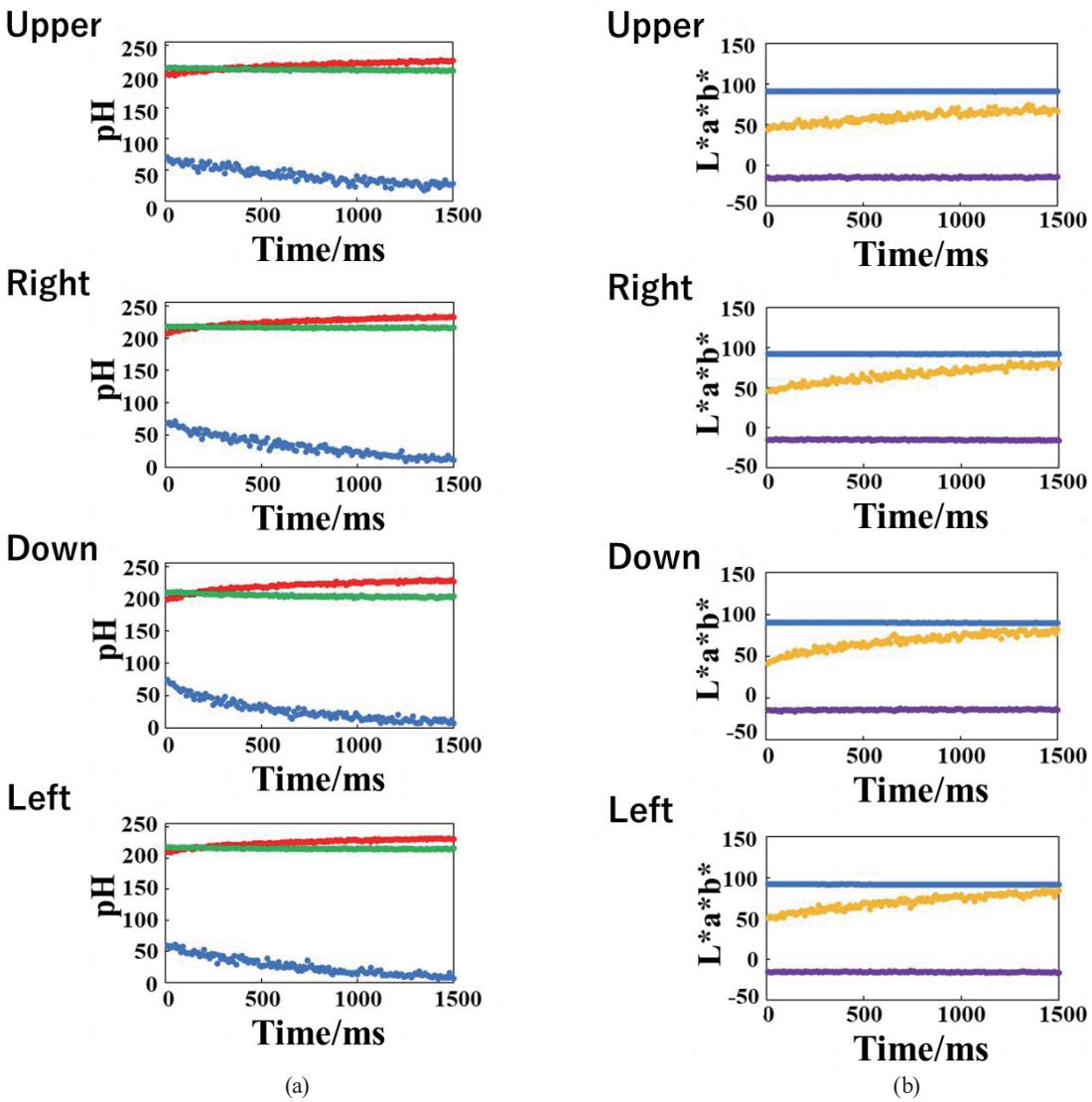

Fig. 7. (Color online) Results of analyzing the images in Fig. 6: (a) RGB and (b) L*a*b* values.

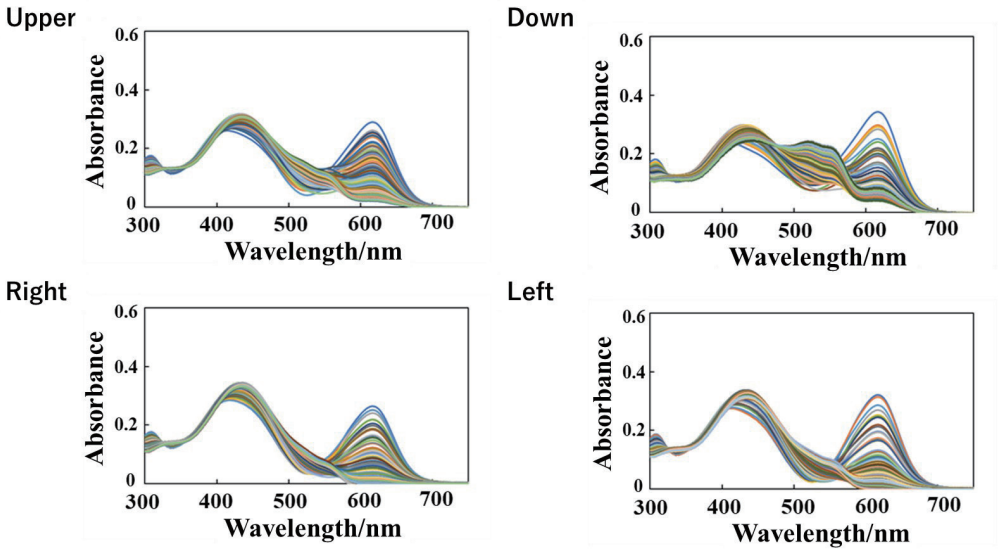

Fig. 8. (Color online) Reproduced absorption spectra of BTB−MR in agarose gel at four points near the ion-exchange resin.

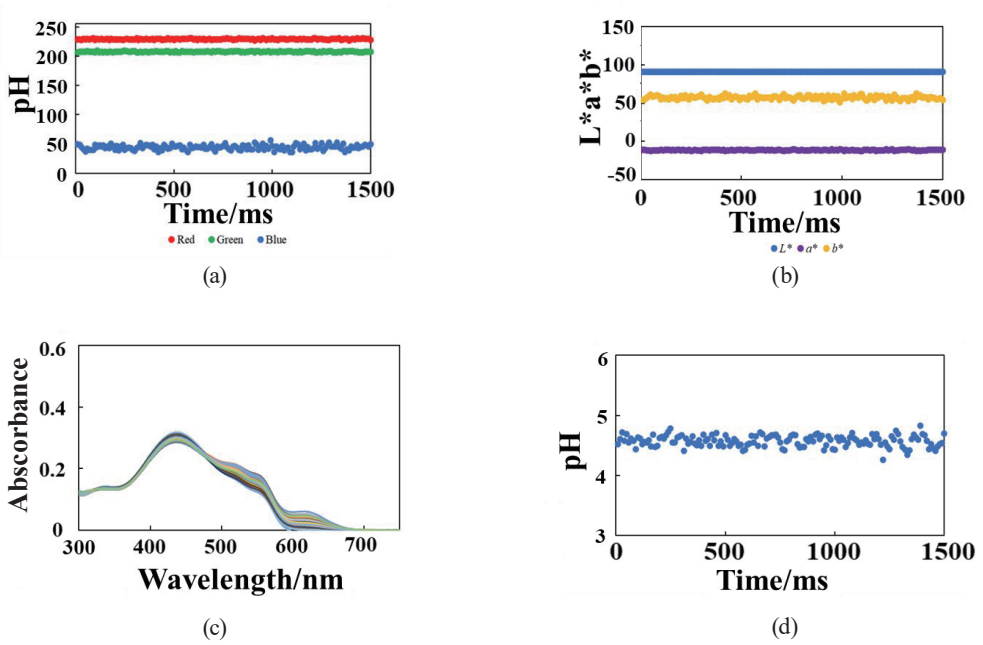

Fig. 9. (Color online) Absorption spectra of BTB−MR solution (pH 4.71) obtained by rapid acquisition: (a) RGB values, (b) L*a*b* values, (c) reproduced absorption spectra every 10 ms for 1500 ms, and (d) pH values obtained with the regression equation.

respectively. The absorption spectra were reproduced using these RGB values, as summarized in Fig. 9(c). The pH values calculated from these spectra using Eq. (4) were in the range from 4.26 to 4.83, as shown in Fig. 9(d). These results confirm both the feasibility of the regression curve and the rapid acquisition of absorption spectra for pH determination. We then applied this regression curve for pH determination to the ion-exchange resin placed on 0.1 wt% agarose gel. The pH values obtained are shown in Fig. 10. Compared with our previous study using BTB,[14] the reproducibility of pH at lower pH values is much improved.

Nomura *et al.* monitored the pH change in proton diffusion phenomena using the same experimental systems.[17] The pH change at the gel-resin interface was monitored with specially designed pH-responsive electrodes with a time interval of 2 min. The concentration of agar in the gel ranged from 1.5 to 5.0 wt%, which is relatively high. On the other hand, the agarose concentration of the gels used in this method is 0.1 wt%, giving the gels more fluidity. Our results indicate that our simple experimental setup and mathematical treatment allow rapid spectrum-based evaluation, which can be used to measure the behavior of nonequilibrium systems.

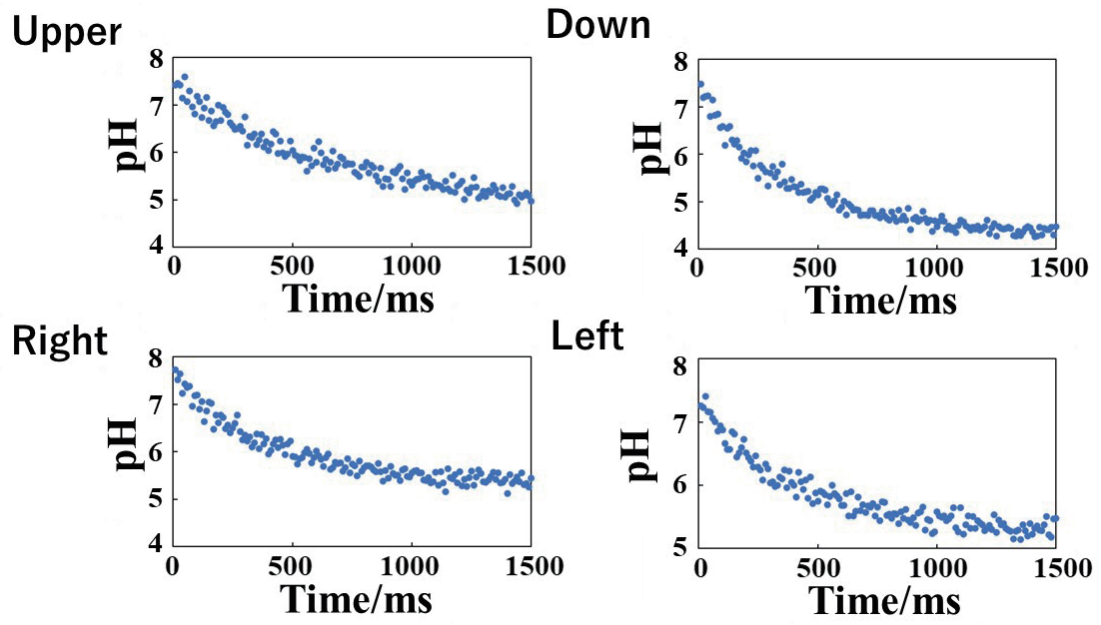

Fig. 10. (Color online) pH values at four points on the BTB−MR−containing agarose gel near the ion-exchange resin.

4. Conclusion

Absorption spectra were reproduced from RGB values of microscopic images of BTB–MR solution taken continuously at 10 ms intervals using the RGB-spectrum conversion method, and pH values were calculated from the reproduced absorption spectra. The variation of the calculated pH values was small. These results indicate that the RGB-spectral conversion method is applicable to ms measurements. To demonstrate the usefulness of this method, the absorption spectra were reproduced from the RGB values of a microscopic image of a gel-resin interface captured immediately after the resin was placed on the gel. pH was calculated from the reproduced absorption spectra. From these results, we were able to quantitatively visualize the interface between the gel and the ion-exchange resin, which changes in a short time of ms order, using the RGB-spectral conversion method. Compared with our previous study, which used only the BTB solution, a wider range of pH values was successfully monitored. The present method, which requires only mathematical processing after image acquisition to obtain the spectra, is expected to be used for the rapid measurement of chemical behavior in the microscopic spaces inside crystals and biological cells. Moreover, the experimental platform is simple compared with the conventional spectroscopy. Thus, we believe that the present method would be one of the novel sensing technologies for the continuous monitoring of spectral change, which can be utilized as precise inline analysis.

Acknowledgments

This work was partially supported by a Grant-in-Aid for Early-Career Scientists (JP19K15599) and a Grant-in-Aid for Scientific Research in Innovative Areas (JP20H05203) from the Japan Society for the Promotion of Science. AI thanks Utsunomiya University for a research grant funded by Utsunomiya University President Strategy Expenses. The authors thank the Advanced Instrumental Analysis Department of Utsunomiya University for instrumental support.

References

1 A. P. Ault: Acc. Chem. Res. **53** (2020) 1703. https://doi.org/10.1021/acs.accounts.0c00303
2 O. Urquidi, J. Brazard, N. LeMessurier, L. Simine, and T. B. M. Adachi: Proc. Natl. Acad. Sci. U. S. A. **119** (2022) 1–8. https://doi.org/10.1073/pnas.2122990119
3 H. Hou, Y. Zhao, C. Li, M. Wang, X. Xu, and Y. Jin: Sci. Rep. **7** (2017) 1. https://doi.org/10.1038/s41598-017-01956-1
4 T. Noguchi, M. Kimura, T. Nakamura, T. Kitajima, A. Tsuchiyama, M. Abe, A. Fujimura, T. Mukai, T. Okada, M. Ueno, T. Yada, Y. Ishibashi, K. Shirai, and R. Okazaki: Bunseki Kagaku. **61** (2012) 299 (in Japanese). https://doi.org/10.2116/bunsekikagaku.61.299
5 H. Hisamoto, T. Saito, M. Tokeshi, A. Hibara, and T. Kitamori: Chem. Commun. (2001) 2662. https://doi.org/10.1039/b106494k
6 M. Numata and C. Kanzaki: Crystals. **8** (2018) 300. https://doi.org/10.3390/cryst8070300
7 J. E. Katon: Micron. **27** (1996) 303. https://doi.org/10.1016/S0968-4328(96)00045-5
8 B. Smits: J. Graph. Tools. **4** (1999) 11. https://doi.org/10.1080/10867651.1999.10487511
9 A. Inagawa, A. Sasaki, and N. Uehara: Talanta. **216** (2020) 120952. https://doi.org/10.1016/j.talanta.2020.120952
10 A. Inagawa, K. Saito, A. Sasaki, and N. Uehara: Data Br. **31** (2020) 105998. https://doi.org/10.1016/j.talanta.2020.120952

11 A. Inagawa, and N. Uehara: Bunseki Kagaku. **69** (2020) 693 (in Japanese). https://doi.org/10.2116/bunsekikagaku.21.1551
12 A. Inagawa, K. Saito, M. Fukuyama, M. Numata, and N. Uehara: Anal. Chim. Acta. **1182** (2021) 338952. https://doi.org/10.1016/j.aca.2021.338952
13 A. Inagawa, M. Kimura, and N. Uehara: Anal. Sci. **38** (2022) 869. https://doi.org/10.1007/s44211-022-00107-5
14 Y. Kimura, A. Inagawa, and N. Uehara: Anal. Sci. **39** (2023) 1425. https://doi.org/10.1007/s44211-023-00348-y
15 D. C. Harris: Quantitative Chemical Analysis, D. C. Harris, Ed. (W. H. Freeman, New York, 2016) 9th ed., Chap. 11.
16 L. S. Foster and I. J. Gruntfest: J. Chem. Educ. **14** (1937) 274. https://doi.org/10.1021/ed014p274
17 S. Nomura, S. Takamatsu, M. Nakao, Y.-G. Yang, C. Inoue, and T. Chida: Bunseki Kagaku. **48** (1999) 763 (in Japanese). https://doi.org/10.2116/bunsekikagaku.48.763